Optimization of Mid to Long Range Flights Considering Air-to-Air Refueling for Fuel Savings

M. Bittner, C. Hornfeck**, F. Fisch***, M. Schwarze**** and F. Holzapfel******
**Research Assistant, Institute of Flight System Dynamics, Technische Universität München, Boltzmannstr. 15, D-85748 Garching, Germany. m.bittner@tum.de*
***Student, Institute of Flight System Dynamics, Technische Universität München, Boltzmannstr. 15, D-85748 Garching, Germany. christoph.hornfeck@gmail.com*
****Researcher, Institute of Flight System Dynamics, Technische Universität München, Boltzmannstr. 15, D-85748 Garching, Germany. fisch@tum.de*
*****Research Assistant, Institute of Aircraft Design, Technische Universität München, Boltzmannstr. 15, D-85748 Garching, Germany. schwarze@tum.de*
******Director, Institute of Flight System Dynamics, Technische Universität München, Boltzmannstr. 15, D-85748 Garching, Germany. florian.holzapfel@tum.de*

Abstract

This article presents the application of aircraft trajectory optimization methods to mid and long range flights considering air-to-air refueling for fuel savings. An optimal control problem is constructed by using models derived from BADA data and by using an aircraft redesign specifically tailored to missions including aerial refueling. To be able to describe the full mission involving multiple aircraft, cross-system constraints are introduced. The resulting problem is solved via direct collocation. Results show that, depending on the specific mission, total fuel reductions of approximately 10-20% can be achieved, respecting the fuel consumption of the tankers, when considering the redesigned aircraft.

Nomenclature

Frames / References

A	=	Aerodynamic Frame / Motion / Force
B	=	Body-Fixed Frame
E	=	Earth-Centered Earth-Fixed Frame
K	=	Kinematic Flight Path Frame / Motion
O	=	North-East-Down Frame (*NED*)
G	=	Center of Gravity / Gravitational Force
CMD	=	Commanded (as index)
R	=	Reference (as index)
P	=	Propulsive Force (as index)
T	=	Total Force (as index)
$\mathbf{T}$	=	Transformation matrix

Aircraft Controls

α	=	Angle of attack
μ	=	Bank angle
δ_T	=	Thrust lever position

Kinematics

λ	=	Geographic Latitude
φ	=	Geographic Longitude
h	=	Altitude above WGS84 Reference
V	=	Kinematic velocity
χ	=	Flight-path course angle
γ	=	Flight-path climb angle
N_φ	=	WGS84 Radius of Prime Vertical
M_φ	=	WGS84 Meridian Radius of Curvature
a	=	Semi-Major axis
e	=	First Excentricity

Forces

$\vec{\mathbf{F}}$	=	Force vector
T	=	Thrust
L	=	Lift
D	=	Drag
Q	=	Aerodynamic side force

Aircraft parameters and Aerodynamics

m	=	Aircraft mass
C_i	=	Aerodynamic coefficient
C_{D0}	=	Zero-lift drag coefficient
C_{Ti}	=	BADA Thrust Model coefficient
ΔT_{ISA}	=	Temperature offset
S	=	Reference area
$\bar{q}$	=	Dynamic pressure
g	=	Gravitational constant
ρ	=	Air density
C_{fi}	=	BADA Fuel Model coefficient
H_G	=	Geopotential Height
r_E	=	Radius of the Earth
a	=	Speed of sound

State Space Modeling

$\mathbf{x}$	=	State vector
$\mathbf{u}$	=	Control vector

Optimal control problem formulation

J	=	Bolza cost function
e	=	Mayer cost function
$\mathbf{p}$	=	Parameters of optimal control problem
L	=	Lagrange cost function
$\boldsymbol{\psi}_0, \boldsymbol{\psi}_f$	=	Initial / Final boundary conditions
$\mathbf{r}$	=	Interior point conditions
$\mathbf{C}_{eq}, \mathbf{C}_{ineq}$	=	Equality / Inequality constraints

Collocation Method

τ_i	=	Discretized time
$\mathbf{X}$	=	Discretized States over time
$\mathbf{U}$	=	Discretized Controls over time
$\mathbf{z}$	=	Optimization parameter vector
$\mathbf{C}$	=	Optimization equality constraint vector

Declaration: $\left(\vec{\mathbf{V}}^{\text{Reference Point}}_{\text{Type of Motion / Source of Force}}\right)^{\text{Reference Frame}}_{\text{Notation Frame}}$

1. Introduction

As air traffic is growing steadily and oil is becoming more and more expensive due to its limited amount all air traffic stakeholders have great interest in reducing fuel consumption of civil airliners. Eurocontrol, for example, gives a long term prognosis in [1] for IFR Movements and for the oil price in four different scenarios. All of these scenarios show a significant increase of both of these values. Moreover, ecological concerns are of growing interest to airlines and customers. One possibility to reduce fuel consumption especially during long range flights that has been discussed in several works during the last years is the use of air-to-air refueling also for civil applications.

Previously conducted work in this field has mainly been driven by Nangia [2], [3], [4], Green [5], [6] and Hahn [7]. Nangia defines multiple efficiency values for measuring the benefits that can be achieved when using air-to-air refueling for civil configurations. Besides, he focuses on the design of new aircraft specifically tailored for long-haul flights using aerial refueling. This means that the aircraft should have more or less the same payload and size as actual long-range planes but have smaller tanks which influence the whole configuration and the aerodynamics. Green and Hahn focus on the calculation of the most efficient range as well as a similar redesign of aircraft as Nangia.

In this paper, aerial refueling scenarios are considered as aircraft trajectory optimization problems and are tackled with the methods commonly used in this field. These optimal control problems are built up using 3-degree-of-freedom aircraft models based on BADA data [8], where available. The models also implement fuel consumption depending on the aerodynamic situation and the current mass. Besides the models of existing aircraft, additional A380 models with reduced range especially tailored for flights during which refueling takes place are introduced. The relevant parameters for these redesigned aircraft are estimated using general aircraft design principles.

The models used to simulate the behavior of the tankers have also been derived from BADA data and fuel consumption models similar to the airliner models are implemented. These fuel consumption models are essential as the optimization of aerial refueling missions only makes sense when considering the total fuel consumed by both the airliners as well as the tankers.

In this work, different refueling scenarios are implemented and solved as optimal control problems which show the maximum savings that could be achieved. To be able to model the refueling of the aircraft, the problems are divided into multiple phases and constraints on the aircraft positions and the phase times are added. These constraints assure that the tankers and the planes keep their necessary distance during refueling and at any other point in time. The time constraints are needed to assure that the tanker and the aircraft to be refueled are at the same location at the same time even after a different number of preceding phases. The resulting infinite optimal control problem is discretized using an Euler-Forward collocation scheme which leads to a finite parameter optimization problem that can be solved using an NLP-solver. In the paper at hand SNOPT is used for that purpose. Moreover, not only scenarios incorporating one flight and one refueling operation are considered but also scenarios with different flights and even multiple refueling operations are investigated.

The paper is divided as follows: Section 2 introduces the aircraft simulation models derived from BADA data while the aircraft redesign for refueling missions is roughly discussed in section 3. Section 4 highlights some of the special aspects of the resulting optimal control problems such as constraints between aircraft positions before section 5 gives an overlook of the Euler Forward collocation method used to discretize the problem, to derive a parameter optimization problem from the nonfinite optimal control problem and the generation of adequate initial guesses. In section 6 the main results for some exemplary refueling missions are presented before in section 7 the adequate conclusions are drawn and a brief outlook is given.

2. Aircraft Simulation Model

The simulation models used in this aircraft trajectory optimization task are extended point mass simulation models either based on the BADA database published by EUROCONTROL [8] or on lookup tables calculated by basic aircraft design principles as presented in section 3. They comprise position equations of motion and translation equations of motion as well as a thrust model, an atmosphere model and a model for the fuel consumption. As the models are controlled by α_{CMD}, μ_{CMD} and $\delta_{T,CMD}$, the required force and load factor equations need to be implemented as well. For the position equations of motion latitude, longitude and height are chosen as WGS84-Coordinates given in the North-East-Down Frame O. Their derivatives are given with respect to the Earth-Centered-Earth-Fixed Frame E:

$$\begin{pmatrix} \dot{\lambda} \\ \dot{\varphi} \\ \dot{h} \end{pmatrix}_O^E = \begin{pmatrix} \dfrac{V_K^G \cdot \cos(\gamma_K^G) \cdot \sin(\chi_K^G)}{\left(N_\varphi + (h)_O\right) \cdot \cos(\varphi)_O} \\ \dfrac{V_K^G \cdot \cos(\gamma_K^G) \cdot \cos(\chi_K^G)}{M_\varphi + (h)_O} \\ V_K^G \cdot \sin(\gamma_K^G) \end{pmatrix}_O^E \tag{1}$$

In equation (1) N_φ denotes the radius of the prime vertical of the WGS84 reference ellipsoid and M_φ its meridian radius of curvature, with a being the semi-major axis and e being the first excentricity:

$$\begin{aligned} N_\varphi &= \frac{a}{\sqrt{1 - e^2 \sin^2(\varphi)_O}} \\ M_\varphi &= N_\varphi \cdot \frac{1 - e^2}{1 - e^2 \sin^2(\varphi)_O} \end{aligned} \tag{2}$$

The translation equations of motion are given with respect to the Kinematic Reference Frame K. The derivatives with respect to time of the Kinematic Flight Path Velocity V_K^G, the Kinematic Course Angle χ_K^G and the Kinematic Flight Path Inclination Angle γ_K^G depend on the total force $\left(\vec{\mathbf{F}}_T^G\right)_K$ acting on the aircraft's center of gravity as follows:

$$\begin{pmatrix} \dot{V}_K^G \\ \dot{\chi}_K^G \\ \dot{\gamma}_K^G \end{pmatrix}_K^{EO} = \frac{1}{m} \cdot \begin{pmatrix} 1 & 0 & 0 \\ 0 & \dfrac{1}{V_K^G \cdot \cos\gamma_K^G} & 0 \\ 0 & 0 & -\dfrac{1}{V_K^G} \end{pmatrix} \cdot \left(\vec{\mathbf{F}}_T^G\right)_K \tag{3}$$

To calculate the total force $\left(\vec{\mathbf{F}}_T^G\right)_K$ (noted in the Kinematic Frame K) containing the Aerodynamic Force $\left(\vec{\mathbf{F}}_A^G\right)_A$ (notated in the Aerodynamic Frame A), the Propulsion Force $\left(\vec{\mathbf{F}}_P^G\right)_A$ (notated in the Aerodynamic Frame A) and the gravitational force. The forces can be evaluated in the respective frame and need to be transformed into the Kinematic Frame K afterwards:

$$\left(\vec{\mathbf{F}}_T^G\right)_K = \mathbf{T}_{KA} \cdot \left(\vec{\mathbf{F}}_T^G\right)_A = \mathbf{T}_{KA} \cdot \left[\left(\vec{\mathbf{F}}_A^G\right)_A + \left(\vec{\mathbf{F}}_P^G\right)_A\right] + g \cdot \begin{pmatrix} -\sin\gamma_K^G \\ 0 \\ \cos\gamma_K^G \end{pmatrix} \tag{4}$$

Lift and drag are modeled in accordance to BADA using linear and symmetric quadratic aerodynamic polars. As no configuration changes are taken into account the models for cruise configuration are used along the whole trajectories.

$$\left(\vec{\mathbf{F}}_A^G\right)_A = \begin{pmatrix} -D \\ Q \\ -L \end{pmatrix}_A = \begin{pmatrix} -\bar{q} \cdot S \cdot C_D \\ 0 \\ -\bar{q} \cdot S \cdot C_L \end{pmatrix}_A = \begin{pmatrix} -\bar{q} \cdot S \cdot \left(C_{D0,CR} + C_{D2,CR} \cdot \left(C_{L,0} + C_{L,\alpha} \cdot \alpha_{CMD}\right)^2\right) \\ 0 \\ -\bar{q} \cdot S \cdot \left(C_{L,0} + C_{L,\alpha} \cdot \alpha_{CMD}\right) \end{pmatrix}_A \tag{5}$$

Thereby, the dynamic pressure $\bar{q}$ is given as:

$$\bar{q} = \frac{1}{2} \cdot \rho \cdot (V_K^G)^2 \tag{6}$$

The thrust force is based on the jet engine model from BADA [8] (if applicable) and interpolated linearly by the thrust lever position:

$$T = \delta_T \cdot T_{max} \tag{7}$$

When considering jet-powered aircraft, the maximum thrust T_{max} required in equation (7) can be calculated at ISA standard atmosphere from the aircraft's altitude in feet according to the following equations:

$$T_{max} = T_{max,ISA} \cdot \left(1 - C_{Tc5} \cdot \Delta T_{ISA,eff}\right) \tag{8}$$

$$T_{max,ISA} = C_{Tc1} \cdot \left(1 - \frac{h}{C_{Tc2}} + C_{Tc3} \cdot (h[ft])_O{}^2\right) \tag{9}$$

When considering temperature deviations from ISA standard atmosphere, the following equations have to hold:

$$\Delta T_{ISA,eff} = \Delta T_{ISA} - C_{Tc4} \tag{10}$$

$$0 \leq \mathrm{C_{Tc5}} \cdot \Delta T_{ISA} \leq 0.4 \tag{11}$$

Also the fuel flow model used can be found in [8]. Herein, the fuel consumption (in kilograms per minute) is computed depending on the actual aerodynamic velocity V_A (given in knots), the altitude of the aircraft h (given in feet), the maximum available thrust T_{max} (in kiloNewtons) and the thrust lever position δ_T. For jet-aircraft, the maximum and idle fuel consumption can be computed by:

$$\dot{m}_{fuel,max} = C_{f1} \cdot \left(1 + \frac{V_A[kts]}{C_{f2}}\right) \cdot T_{max} \tag{12}$$

$$\dot{m}_{fuel,idle} = C_{f3} \cdot \left(1 - \frac{(h[ft])_O}{C_{f4}}\right) \tag{13}$$

To calculate the actual fuel flow from the maximum and the idle fuel flow given in equations (12) and (13) a linear interpolation with respect to the thrust lever position is implemented:

$$\dot{m}_{fuel} = \dot{m}_{fuel,idle} + \delta_T \cdot \left(\dot{m}_{fuel,max} - \dot{m}_{fuel,idle}\right) \tag{14}$$

The differential equation for the aircraft mass is then given by:

$$\dot{m} = -\dot{m}_{fuel} \tag{15}$$

For the newly created aircraft types also considered in this paper, of course, no BADA data is available. Therefore, a basic redesign study has been conducted as presented in the following section. One of the results of this study is a lookup table containing information about an aircraft's thrust and the corresponding fuel flow depending on the current altitude, the thrust lever position and the Mach number. This information is approximated by a continuously differentiable spline representation by which also all gradients can be calculated. Figure 1 and Figure 2 exemplarily show part of the data used.
The atmospheric data needed such as static pressure, static air temperature and density is calculated using the International Standard Atmosphere (ISA) DIN ISO 2533 [9], where also deviations from this standard atmosphere model can be taken into account. First, the geopotential height H_G is computed from the radius of the Earth r_E and the geodetic height h:

$$H_G = \frac{r_E \cdot h}{r_E + h} \tag{16}$$

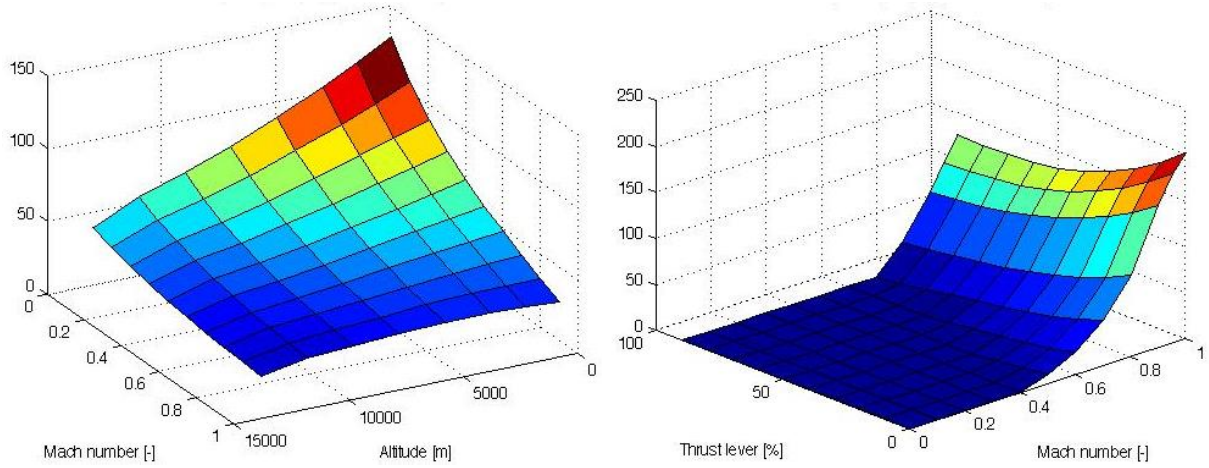

Figure 1: Exemplary lookup table data used for the thrust model.
Left: Thrust per Engine [kN] at thrust lever position 80%. Right: Thrust per Engine [kN] at altitude 5000m.

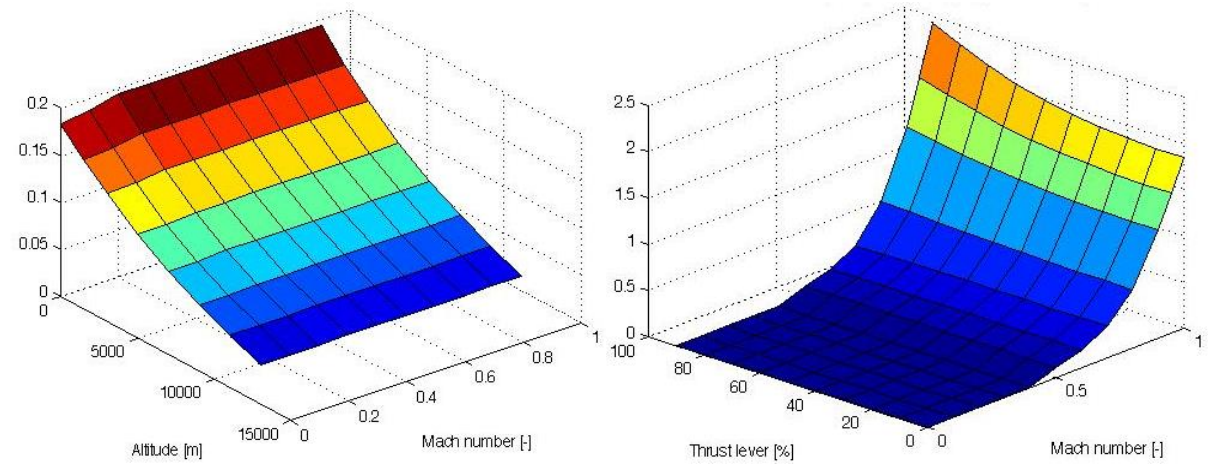

Figure 2: Exemplary lookup table data used for the fuel flow model.
Left: Fuel flow per Engine [kg/s] at thrust lever position 50%. Right: Fuel flow per Engine [kg/s] at altitude 5000m.

When only considering flights with geopotential heights being smaller or equal to the maximum height for the troposphere layer, meaning $H_G \leq 11000m$, the air density ρ and the static pressure p are computed as:

$$\rho = \rho_S \cdot \left(1 + \left(\frac{\gamma_{TR}}{T_S}\right) \cdot H_G\right)^{\left(-\frac{g_S}{R \cdot \gamma_{TR}} - 1\right)} \tag{17}$$

$$p = p_S \cdot \left(1 + \left(\frac{\gamma_{TR}}{T_S}\right) \cdot H_G\right)^{\left(-\frac{g_S}{R \cdot \gamma_{TR}}\right)} \tag{18}$$

Here, γ_{Tr} is the temperature gradient of the polytropic troposphere layer and R the specific gas constant. g_S, T_S, ρ_S and p_S indicate the gravitational acceleration, the temperature, the density and the pressure at mean sea level (MSL).
The speed of sound required for the thrust model based on lookup tables and for Mach-number path constraints can be calculated from the atmospheric parameters as:

$$a = \sqrt{\kappa \cdot R \cdot (T_S + \gamma_{Tr} \cdot H_G)} \tag{19}$$

Summing up, in all models used, the state vector comprises three position states, three velocity states and the aircraft mass. This leads to state vectors $\mathbf{x}_i \in \mathbb{R}^7 \forall i \in [1 \ldots N]$ with i being the index of the current aircraft.

3. Redesign of a Long Haul Aircraft for Aerial Refueling

The following section gives a brief overview of the redesign of an Airbus A380 for short to mid-range flights not exceeding 3000nm that could be used for aerial refueling missions. Assuming that carriers wanted to offer existing connections but with the benefits of aerial refueling, they would require aircraft being able to carry the same amount of payload but only over a far shorter distance. The approximate calculation of masses and aerodynamic parameters for such a plane has been conducted at the Institute of Aircraft Design at the Technische Universität München.
As a starting point, the following assumptions have been made: The newly designed A380 will have the same payload, fuselage weight and design point (by means of thrust/weight ratio and area loads) as the existing one. Moreover, the basic performance requirements like cruise speed or T/O landing distance remain the same. First of all, the original A380 has been recalculated to validate the underlying numerical models. The main results of this recalculation can be found in Table 1.
The general relations behind the redesign of the A380 for short range are as follows: The desired reduction in maximum range requires less fuel capacity which also significantly reduces the overall weight when considering unchanged payload. As this means that only the fuel weight portion decreases, all other mass ratios, consisting of the share of structural weight and the share of payload for the plane have to rise as compensation. Both, the overall mass change and the mass relation shift make the required lift drop and hence allow the use of smaller wings in terms of area which also results in a reduced weight of the wings, although they have to be reinforced because of the decreased amount of fuel inside. This, in reverse, shifts the structural weight and its share again such that the problem has to be solved iteratively.
The procedure for the calculation of the required masses, the thrust and the aerodynamic parameters is divided into three major parts that can be seen in Figure 3. The central element of the algorithm is the calculation of the weights and their shares based on a given Maximum Take-Off Weight (MTOW) and the required fuel weight and payload. Therein, the overall structural weight, the Zero Fuel Weight (ZFW) and the weight of the aircraft components are estimated recursively based on general aircraft design principles as they can for example be found in [10], [11], [12] and [13]. For the fuel calculation the BADA Fuel Calculator and the aircraft performance program Piano-X have been used. The reference area – that can be calculated from the weight easily when assuming that the area loading remains unchanged – and the ZFW from the main calculation are fed into a separate algorithm which estimates the wing weight based on [10]. The result generated there is afterwards compared to the result of the main computation. The whole process can be terminated when a given tolerance in the results is reached. Thereafter, the masses and the wing area are fed into the last part of the algorithm that assesses the basic aerodynamic parameters as well as the required thrust based on the similarity of the aircraft performance. This includes the design point in terms of area loading and thrust/weight ratio as well as the specific fuel consumption.

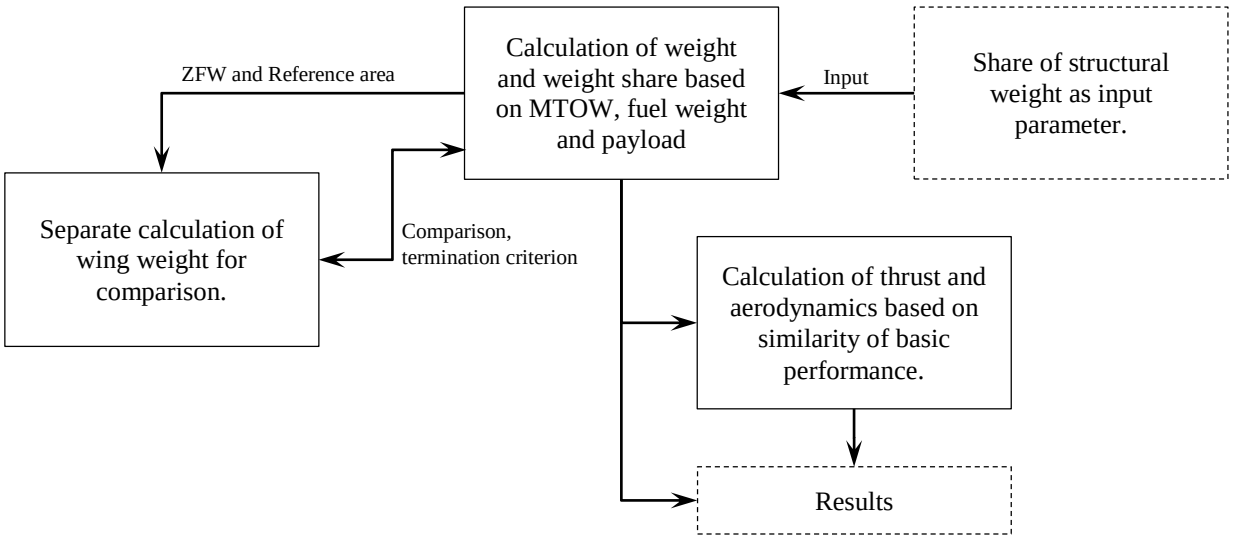

Figure 3: Structure of the calculation process of aircraft masses and parameters

The procedure described above has been performed for two different redesigns of the A380. The first one (A380-388) is tailored for a payload of 59 t (which is the design payload of the original A380-800) and therefore has a maximum

take-off weight of 388t. The second approximation (A380-457) was done for a version designed to carry a payload of about 90t (the maximum payload of the original A380-800) resulting in a Maximum Take-Off Weight of 457t. Table 1 lists the basic parameters for the original A380-800, for the recalculation that was used to verify the model and the two new redesigns for a shortened range of 3000 nm. The data required for the redesign are taken from [14].

Table 1: Basic data of the different A380 redesigns

		A380-800 Original	**A380-800 Evaluation**	**A380-388 (59t payload)**	**A380-457 (90t payload)**
Maximum take-off weight (MTOW)	kg	569000	568390	388000	457000
Operating weight empty (OWE)	kg	270364	270600	226790	247770
Maximum fuel weight	kg	253938	252020	101250	119570
Wing reference area	m²	845	845	608	719
Range	nm	7700	7700	3000+R	3000+R
Payload	kg	59000	59110	59000	90000
C_{L0}		n.p.	5.24	5.51	5.51
$C_{L\alpha}$		n.p.	0.2744	0.2885	0.2885
C_{D0}		n.p.	0.015	0.017	0.016
C_{D2}		n.p.	0.051	0.045	0.045

4. Multi-Aircraft Optimization Problem

When treating multiple aircraft in the context of one aircraft trajectory optimization problem their states and controls have to be concatenated to build up the overall optimal control problem. With i being the index for of one of N aircraft this can generally be formulated as:
Determine the optimal control histories

$$\mathbf{u}_{i,opt}(t) \in \mathbb{R}^{m_i}, \qquad i = 1 \dots N \tag{20}$$

the corresponding optimal state trajectories

$$\mathbf{x}_{i,opt}(t) \in \mathbb{R}^{n_i}, \qquad i = 1 \dots N \tag{21}$$

and all relevant parameters

$$\mathbf{p}_{i,opt} \in \mathbb{R}^{k_i}, \qquad i = 1 \dots N \tag{22}$$

that minimize the overall Bolza cost functional

$$J = \sum_{i=1}^{N} \left[e_i\left(\mathbf{x}_i\left(t_{f,i}\right)\right) + \int_{t_{o,i}}^{t_{f,i}} L_i\left(\mathbf{x}_i(t_i), \mathbf{u}_i(t_i), t_i\right) dt_i \right] \tag{23}$$

subject to all state dynamic equations

$$\dot{\mathbf{x}}_i(t_i) = \mathbf{f}_i(\mathbf{x}_i(t_i), \mathbf{u}_i(t_i), \mathbf{p}_i, t_i), \qquad i = 1 \dots N \tag{24}$$

the initial and final boundary conditions, that now are of combined form

$$\boldsymbol{\psi}_0\left(\mathbf{x}_i\left(t_{0,i}\right), \mathbf{p}_i, t_{0,i}\right) = 0, \qquad i = 1 \dots N \tag{25}$$

$$\boldsymbol{\psi}_f\left(\mathbf{x}_i\left(t_{f,i}\right), \mathbf{p}_i, t_{f,i}\right) = 0, \qquad i = 1 \dots N \tag{26}$$

the interior point conditions

$$\mathbf{r}\left(\mathbf{x}_i\left(t_{k,i}\right), \mathbf{p}_i, t_{k,i}\right) = 0, \qquad i = 1 \dots N \tag{27}$$

as well as equality and inequality path constraints, containing information from all involved systems

$$\mathbf{C}_{eq}(\mathbf{x}_i(t_i), \mathbf{u}_i(t_i), \mathbf{p}_i, t_i) = 0, \qquad i = 1 \dots N \tag{28}$$

$$\mathbf{C}_{ineq}(\mathbf{x}_i(t_i), \mathbf{u}_i(t_i), \mathbf{p}_i, t_i) \leq 0, \qquad i = 1 \dots N \tag{29}$$

It is important here to mention, that all constraints not resulting solely from the dynamics of one single aircraft may depend on all other or at least some of the other aircraft involved. This leads to a highly interdependent optimal control problem.
The following paragraphs describe the specific problem to be solved in more detail. First of all, when using the model from section 2, each airliner as well as each tanker has a state vector containing seven states and a control vector containing three controls of the following form:

$$\mathbf{x}_i = \left[\lambda_i, \phi_i, h_i, V_{K,i}^G, \chi_{K,i}^G, \gamma_{K,i}^G, m_i\right]^T \tag{30}$$

$$\mathbf{u}_i = \left[\alpha_{CMD,i}, \mu_{CMD,i}, \delta_{T,CMD,i}\right]^T \tag{31}$$

As the minimization of the overall fuel consumption of all aircraft involved in the mission is the goal of the optimization, the cost function for the optimal control problem can be formulated as the sum over the differences of each aircraft's initial and its final mass:

$$J = \sum_{i=1}^{N} m_i\left(t_{0,i}\right) - m_i\left(t_{f,i}\right) \tag{32}$$

This is equivalent to the fuel consumption of all airliners and all tankers involved in the scenario. When considering the reference scenarios without refueling of course only the fuel consumed by the airliners appears in the cost function. To keep the aircraft trajectories realistic and flyable, control boundaries and state boundaries are introduced. Firstly the angle of attack α_{CMD} has to remain in between a lower and an upper bound:

$$\alpha_{min} \leq \alpha_{CMD} \leq \alpha_{max} \tag{33}$$

α_{min} and α_{max} have been chosen to $\alpha_{min} = -5.73°$ and $\alpha_{max} = 20.05°$ for the planes considered in the examples below. The bank angle μ_{CMD} of the aircraft is limited by the envelope and the passenger comfort to values between $+45°$ and $-45°$. As the thrust lever position $\delta_{T,CMD}$ is a normalized control it has to remain between 0 and 1:

$$-45° \leq \mu_{CMD} \leq 45° \tag{34}$$

$$0 \leq \delta_{T,CMD} \leq 1 \tag{35}$$

Moreover, path constraints for the load factors $(n_z)_B$ in the vertical plane of the aircraft are applied due to passenger comfort:

$$0.85 \leq (n_z)_B \leq 1.15 \tag{36}$$

For the velocity, aircraft specific upper and lower bounds have to be applied to the calibrated airspeed to account for the flight envelope by means of stalling and buffeting. Moreover, the Mach number is limited for the same reasons:

$$V_{CAS,min} \leq V_{CAS} \leq V_{CAS,max} \tag{37}$$

$$Ma \leq 0.85 \tag{38}$$

Besides the path constraints, also the initial and final boundary conditions of each aircraft have to be applied. Here, the latitude λ_i, longitude ϕ_i and the altitude h_i of the aircraft are set to the corresponding values of their starting and destination airports. As starting and landing are not modeled in a very detailed way with e.g. not considering configuration changes here, the value for the initial and final course angle $\chi^G_{K,i}$ is set to the direction of the runway, and $\gamma^G_{K,i}$ is set to $+3°$ or $-3°$ at the initial or final time to approximate the climb out and the glideslope. The initial mass of each aircraft $m_{0,i}$ is limited between the maximum take-off mass and the zero fuel mass of the aircraft and is subject to optimization.
All previously detailed constraints always affect only one aircraft. To ensure separation between two aircraft a distance constraint is introduced that has to hold for any combination of aircraft $AC1$ and $AC2$ as long as they are not a tanker and an airliner currently refueling:

$$d_{min} \leq \sqrt{\left((\lambda_{AC1} - \lambda_{AC2}) \cdot R_E\right)^2 + \left((\phi_{AC1} - \phi_{AC2}) \cdot R_E\right)^2 + (h_{AC1} - h_{AC2})^2} \tag{39}$$

For simplicity, the Euclidian Norm has been used as separation measure here. The limit d_{min} for the distance between two aircraft has been set to $d_{min} = 5000\ m$ in the examples below.
In that phases of the problem where the refueling takes place, the position of the aircraft to be refueled and that of the tanker refueling have to be close enough such that the refueling is technically possible. In the problems considered here, for simplicity, the positions of these two aircraft are set equal during refueling:

$$\begin{aligned} \lambda_{AC1} &= \lambda_{AC2} \\ \phi_{AC1} &= \phi_{AC2} \\ h_{AC1} &= h_{AC2} \end{aligned} \tag{40}$$

To be able to model whole flights including refueling, a phase approach has been chosen. This means that each trajectory is divided into several phases of time $T_{Xi,j}$, where every second phase is a refueling phase and every other phase is a normal travel flight phase. Figure 4 depicts an example with two airliners traveling from left to right each being refueled twice. For the airliners, odd phases are pure travel flight phases, which for the tankers are phases where they either travel from their base airport to the first airliner, from one airliner to the next or back to their base. For both, the tankers and the airliners, the even phases are the refueling phases. The length of this refueling phase has to have the same duration for the airliner as for the tanker, which is assured by the following parameter constraint:

$$T_{Ai,2j} = T_{Tj,2i} \tag{41}$$

Besides the equality of the times in the refueling phases, also the times between two refuelings have to be equal. To assure this the following phase time constraint is introduced:

$$T_{Ai,2j+1} + T_{Ai,2j+2} + T_{Tk+1,2i+1} = T_{Tk,2i+1} + T_{Ai+1,2j} + T_{Ai+1,2j+1} \tag{42}$$

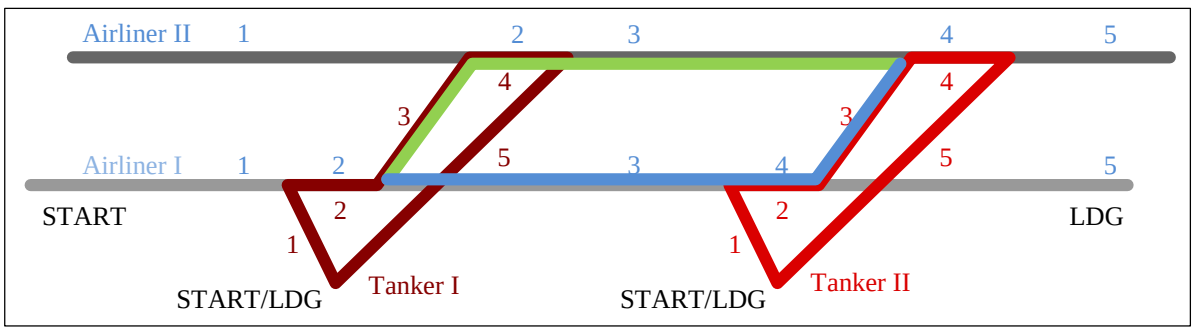

Figure 4:Phase times and their parameter dependencies between two refueling maneuvers.

Here, the first index enumerates the aircraft (A) or Tanker (T) considered, followed by the number of the relevant phase, where i is the index of the aircraft, j is the index of the refueling maneuver and k is the index of the tanker. shows this constraint in a two-aircraft-two-tanker scenario. The sum of phase times along the blue path – which is the left side of equation (42) – has to be the same as the sum of phase times along the green path – which is the right side of equation (42).

5. Discretization Method

The optimal control problem described above is discretized using Euler Forward Collocation as it can for example be found in Betts [15] and [16]. Therefore, firstly the overall simulation time has to be discretized with the step size h:

$$\tau_i = t_0 + (i-1) \cdot h \tag{43}$$

The discretization of the states and the controls at the time discretization points given in (43) leads to a finite set of state and control variables:

$$\mathbf{X} = \{\mathbf{x}_i\}, \quad \mathbf{U} = \{\mathbf{u}_i\} \tag{44}$$

To ensure that the dynamic equations describing the aircraft's behavior are fulfilled at least at the discretization points the Euler Forward integration scheme

$$\mathbf{x}_{i+1} = \mathbf{x}_i + h \cdot \mathbf{f}(\mathbf{x}_i, \mathbf{u}_i, \mathbf{p}) \tag{45}$$

is applied and reformulated such that it can be added to the problem as additional equality constraints:

$$\mathbf{x}_{i+1} - \mathbf{x}_i - h \cdot \mathbf{f}(\mathbf{x}_i, \mathbf{u}_i, \mathbf{p}) = \mathbf{0} \tag{46}$$

This leads to a discretized optimal control problem of the following form:
Find the optimal parameter vector containing the optimal states and controls

$$\mathbf{z} = [\mathbf{X}, \mathbf{U}]^T \tag{47}$$

that minimizes the cost function

$$J(\mathbf{z}) \tag{48}$$

subject to the discretized inequality conditions

$$\mathbf{C}_{ineq}(\mathbf{X}(\mathbf{z}), \mathbf{z}) \leq \mathbf{0} \tag{49}$$

as well as the discretized equality conditions

$$\mathbf{C} = \begin{pmatrix} \boldsymbol{\psi}_0(\mathbf{X}(\mathbf{z}), \mathbf{z}) \\ \mathbf{C}_{eq}(\mathbf{X}(\mathbf{z}), \mathbf{z}) \\ \mathbf{x}_{i+1} - \mathbf{x}_i - h \cdot \mathbf{f}(\mathbf{x}_i, \mathbf{u}_i, \mathbf{p}) \\ \mathbf{r}(\mathbf{X}(\mathbf{z}), \mathbf{z}) \\ \boldsymbol{\psi}_f(\mathbf{X}(\mathbf{z}), \mathbf{z}) \end{pmatrix} = \mathbf{0} \tag{50}$$

containing the initial boundary conditions $\boldsymbol{\psi}_0$ the equality path constraints $\mathbf{C}_{eq}$ the constraints originating from the discretized dynamics as well as the interior point conditions $\mathbf{r}$ and the final boundary conditions $\boldsymbol{\psi}_f$. The resulting

finite dimensional parameter optimization problem can be solved using an NLP-solver, where in the examples considered, SNOPT [17] is used for that purpose.
Whenever using a local optimization algorithm such as the gradient based method implemented in SNOPT a good initial guess is required to achieve fast and reliable convergence. For that purpose in the examples presented great circles are generated from the airport positions of the start and the destination and used as initial guesses for latitude and longitude. The course angle can then be calculated from that tracks. The initial height profile is approximated by a straight segment at $h = 11000m$ and an adequate climb and decent segment with γ=±3°. No values for the controls are estimated as they are not so important when using a full discretization approach such as collocation. Nevertheless, this can be done by dynamic inversion if necessary.

6. Results

Multiple scenarios have been investigated using the methods described above, where two are presented in more detail here. Afterwards, some general trends that have been realized will be pointed out very briefly.
The first example only involves one aircraft, for which an Airbus A380 has been chosen. The flight considered is intended to go from Munich in Germany (MUC) to Sao Paulo in Brazil (GRU). For the reference mission without refueling the model of a regular A380 is used. For the flight with refueling the redesigned A380-388 with a shorter range of 3000nm has been used as airliner, while a model of a Boeing KC767-300 has been used as tanker. The tanker base was located at Ad-Dakhla in Marocco (VIL). Table 2 lists the initial and final positions and headings for the airliner as well as the tanker.

Table 2: Initial and final conditions for an example flight from
Munich, Germany (MUC) to Sao Paulo, Brazil (GRU), Tanker based in Ad-Dakhla, Marocco (VIL)

AC	**A380 / A380-388**	**KC 763**
λ_0	11.7510°E	15.9320°W
φ_0	48.3407°N	23.7183°N
h_0	453 m	11 m
χ_0	263°	30°
λ_f	46.4695°W	15.9320°W
φ_f	23.4320°S	23.7183°N
h_f	750 m	11m
χ_f	254°	30°

In Figure 5 the optimized trajectory for the flight can be seen in an Eckert-Projected map of the earth. The tanker basis is located in the black circle, which also leads to an optimized refueling maneuver located near there.

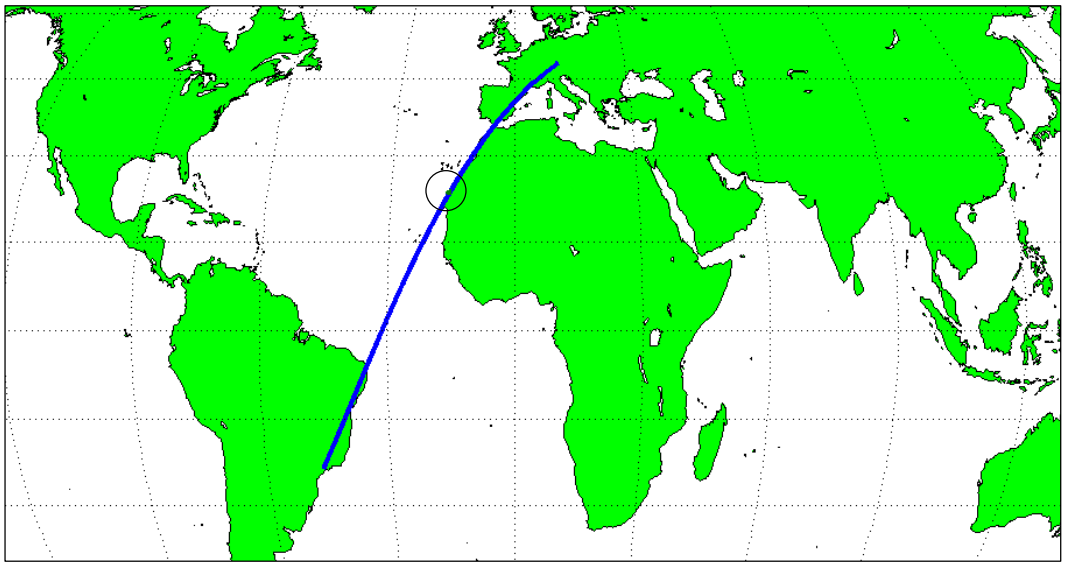

Figure 5: Optimized trajectory for the exemplary flight from MUC to GRU with refueling by a tanker based in VIL.

The controls resulting from the optimization can be seen in Figure 6 (left) where only the time segment in which the refueling takes place is plotted as the controls remain mainly constant along the rest of the trajectory. It can clearly be seen at which time the tanker is starting its refueling mission and that the actual refueling maneuver roughly takes place between $t = 1.58 \times 10^4 s$ and $t = 1.71 \times 10^4 s$. In that phase, the angle of attack of the tanker (upmost graph, green line) needs to be corrected continuously as the weight of tanker is decreasing very quickly. The right plot of Figure 6 depicts the fuel masses onboard the two aircraft during the flights. One can recognize that the airliner does not start with full fuel as this would not result in the minimum fuel efficiency of that flight but only has enough fuel onboard to reach the tanker.

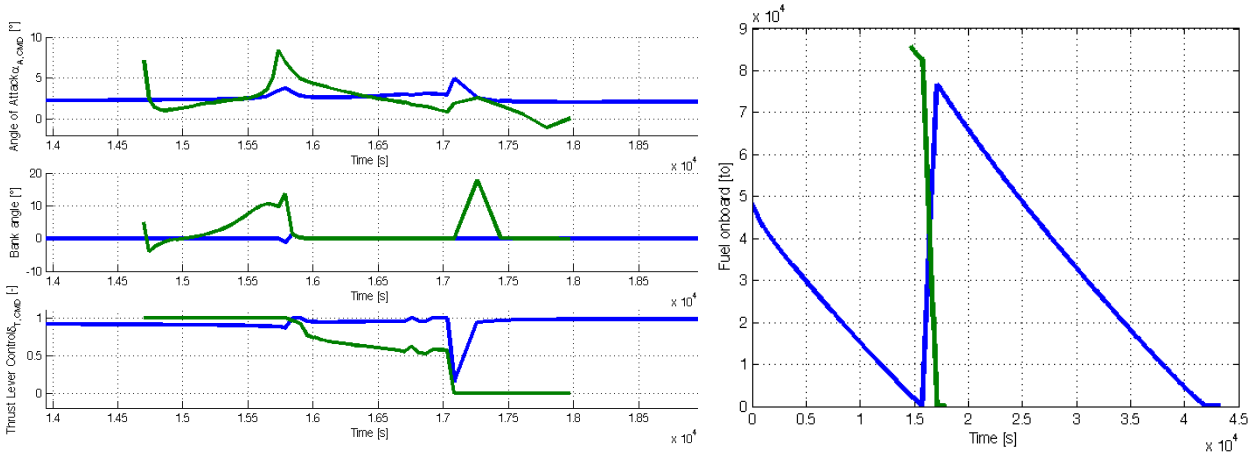

Figure 6: Relevant time segment of optimized controls (left) and
resulting fuel masses onboard the airliner and the tanker (right) for flight from MUC to GRU
with refueling near VIL. Blue line: airliner, green line: tanker.

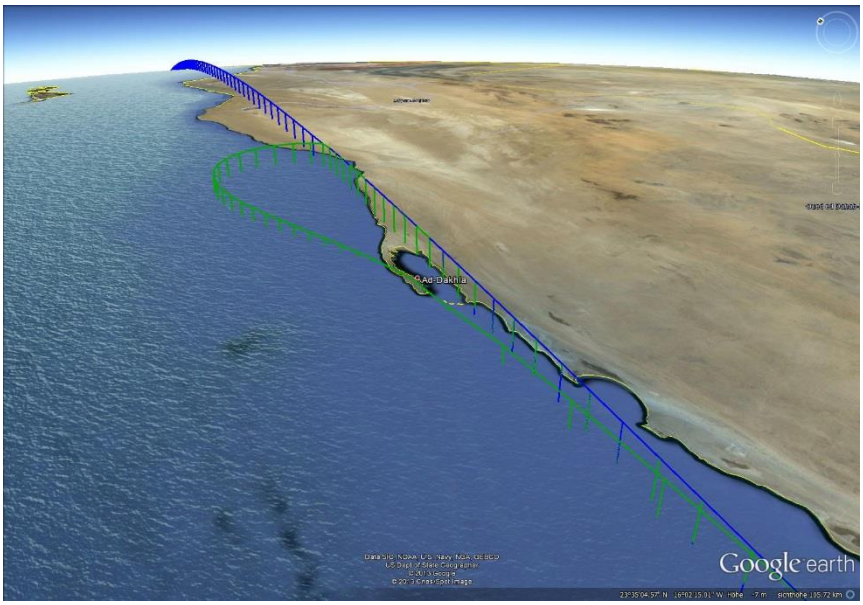

Figure 7: Optimized refueling maneuver for the exemplary flight from MUC to GRU near VIL.

Figure 7 is an image created in Google Earth showing the trajectories while the refueling maneuver takes place. It can be seen how the tanker climbs up until it reaches the airliner before both fly synchronously for a certain distance the airliner receiving the fuel. Afterwards the tanker descends to return to its base airport.
In this example fuel savings of approximately 14% could be achieved by aerial refueling. While the regular Airbus A380 consumed approximately 156t of fuel in the simulation, the redesigned A380-388 only consumed 127t of fuel. Of course, the fuel consumption of the tanker also has to be taken into account which was roughly 7t in the example

simulation. Overall, without refueling, 156t of fuel were used while with refueling only 134t of fuel have been burnt which is a reduction to 85.8%.
The second example presented involves two airliners: one flying from Munich in Germany (MUC) to San Francisco in the USA (SFO) and another one going from Frankfurt in Germany (FRA) to Los Angeles in the USA (LAX). In the reference scenario, once again, for both flights A380 models are used, while for the refueling scenario, the redesigned A380-388 models have been used. In the latter calculations another Airbus A380 is used as a tanker, considering all its payload to be fuel, stationed in Sisimiut in Greenland (JHS). Table 3 lists the initial and final conditions for the two flights and the tanker.

Table 3: Initial and final conditions for two example flights from Munich, Germany (MUC) to San Francisco, USA (SFO), and Frankfurt, Germany (FRA) to Los Angeles, USA (LAX) Tanker based in Sisimiut, Greenland (JHS)

AC	**A380 (MUC-SFO)**	**A380 (FRA-LAX)**	**A380 T**
λ_0	11.7510°E	8.5342°E	53.7293°W
φ_0	48.3407°N	50.1428°N	66.9513°N
h_0	453 m	100 m	9 m
χ_0	263°	250°	62°
λ_f	122.3807°W	118.4190°W	53.7293°W
φ_f	37.6068°N	33.9338°N	66.9513°N
h_f	3 m	36 m	9 m
χ_f	208°	263 °	62°

The optimized flight paths of the three aircraft can be seen on a map of the earth in Eckert Projection in Figure 8, where the first flight going from MUC to SFO is depicted in blue, the second flight going from FRA to LAX is depicted in green and the trajectory of the tanker stationed in JHS is printed in red.

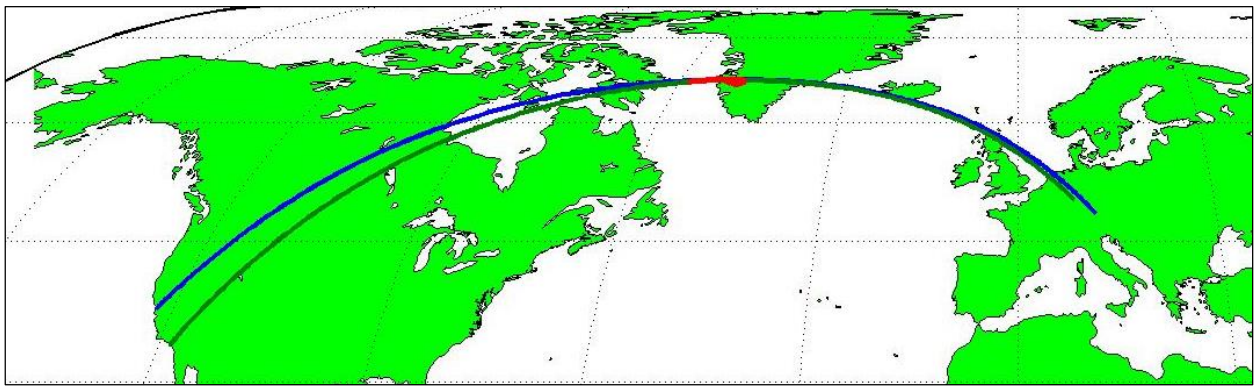

Figure 8: Optimized example flights with aerial refueling for MUC-SFO (blue), FRA-LAX (green) and a tanker based in JHS (red).

Figure 9 shows the optimized controls for the second example and Figure 10 shows the fuel onboard of each of the aircraft. What can be seen in the latter is that the tanker in this example cannot carry enough fuel to refuel both aircraft completely for their remaining routes. This leads to an optimized solution where the second aircraft does not start with the minimum amount of fuel required until the refueling (the aircraft still has fuel left), but with the minimum fuel required for the first segment plus that part of the last segment that cannot be received by the tanker.

Table 4: Results for the second example by means of fuel consumption.

Fuel Consumption	**Without refueling**	**With refueling (and redesign)**
A380 (MUC-SFO)	149 t	118 t
A380 (FRA-LAX)	147 t	129 t
A380 Tanker	---	20 t
Sum	296 t	267 t

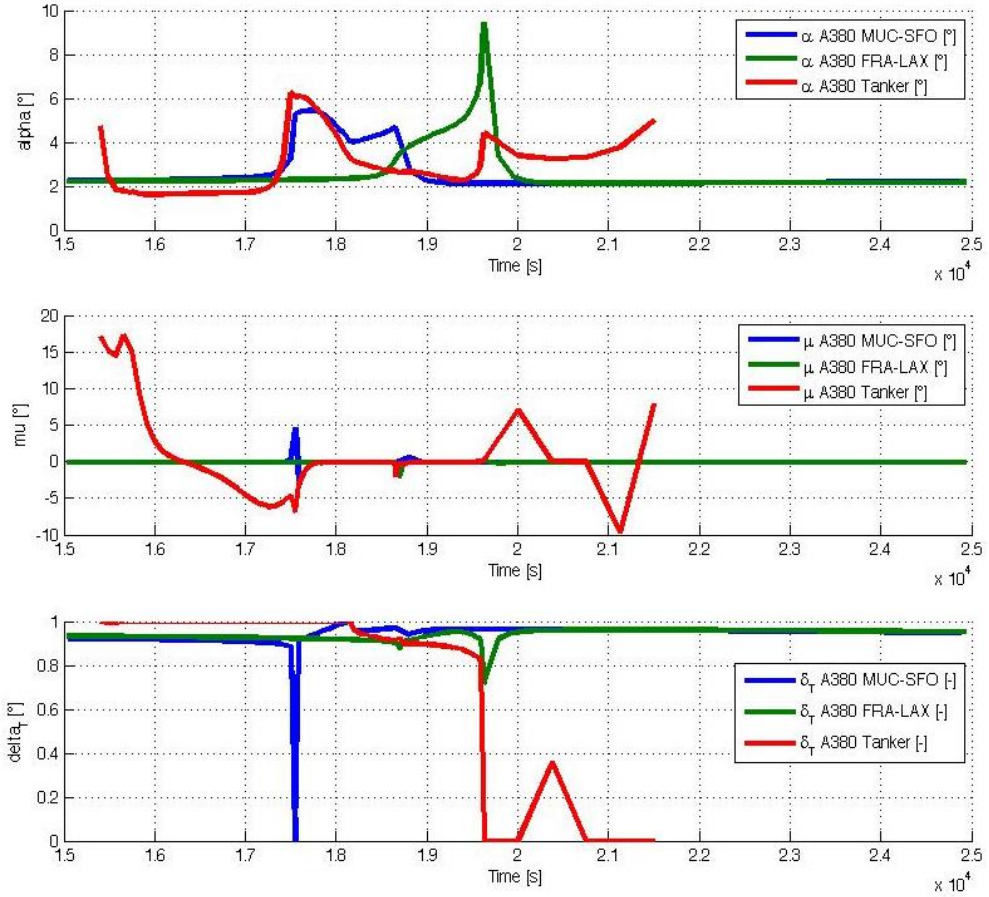

Figure 9: Optimized controls for all three aircraft of the second example over time. Only the timespan where the refueling takes place is shown.

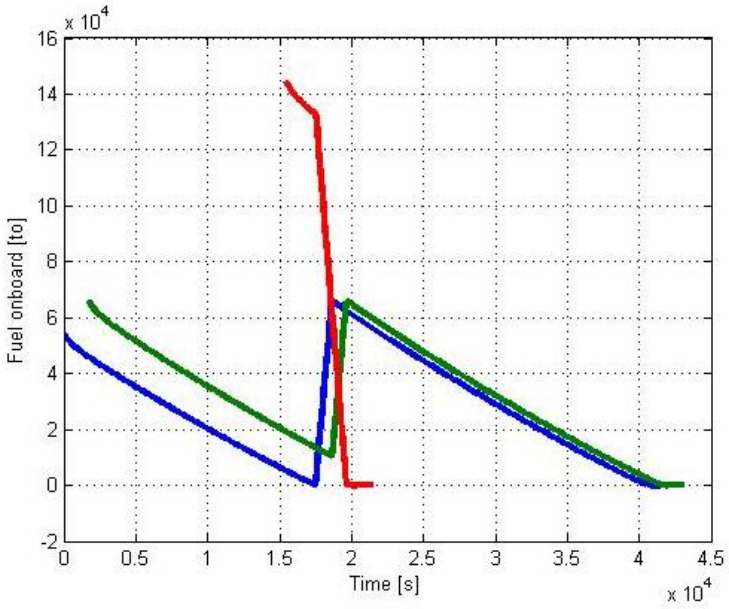

Figure 10: Fuel Consumption during second example flight from MUC to SFO (blue) and FRA to LAX (green), tanker based in JHS (red).

The overall savings that could be achieved in the second example are listed in Table 4. The two overseas flights in the simulation consumed 296t of fuel, while the flights using the redesigned models and being refueled only burnt 247t of fuel. In this case, an additional 20t of fuel was needed for the tanker which in total leads to a reduction of fuel consumption of approximately 9.8% or 29t.
During the overall investigations on aerial refueling for civil applications in the context of aircraft trajectory optimization at the Institute of Flight System Dynamics at TU München, generally fuel savings due to refueling have been in an approximate range of 5% to 20%. Thereby, without redesigning the aircraft fuel savings of approximately 5-7% could be achieved, while another 5-10% could be achieved when also redesigning the airliner for shorter ranges. Overall, the achievable savings very strongly depend on the mission profiles to be optimized and on the size of the tanker aircraft. Moreover, the number of refueling maneuvers per flight and per tanker have a strong influence on the results of the optimization.

7. Summary & Outlook

In the paper at hand, civil aerial refueling missions for fuel savings have been investigated using methods from the field of optimal control. Therefore, trajectory optimization problems involving multiple aircraft have been set up and solved. For the airliners as well as the tankers models derived from BADA and models developed using general principles of aircraft design have been used. The latter are modifications of existing long haul planes specifically tailored for refueling missions.
To be able to solve the problem at hand using optimal control methods, path constraints have been introduced that ensure separation between the aircraft while not refueling besides constraints that keep the aircraft in formation during refueling. After discretization of the whole optimal control problem using the Euler Forward Collocation approach the resulting parameter optimization problems have been solved using the commercial NLP-algorithm SNOPT.
The results for two exemplary mid to long range flights with and without refueling have been presented, where fuel reductions of up to 5% can be achieved by aerial refueling without changing the configuration of the aircraft and a reduction of approximately 10-20% is possible when using configurations specifically tailored for refueling. In all cases the overall fuel burnt is used as cost function, meaning that also the fuel burnt by the tanker aircraft has been taken into account.
In the examples presented here, the tanker basis has been chosen in advance and was not subject to optimization. This would be one possible enhancement for future research on the topic. It is expected to save even more fuel, when the placement of the tanker's basis is optimized. Here, two possible versions might be investigated as one might consider only existing airports or all possible airport locations. Moreover, no safety constraints like reserve fuel remaining onboard each aircraft are considered in this work. These constraints would in some way be dynamic, when considering refueling scenarios, as the refueling maneuver itself may fail and the remaining fuel should nevertheless always be sufficient to return to a safe airport. This would lead to constraints on the remaining fuel at each point in time depending on the distance to the nearest suitable airport. Furthermore, the distance path constraints could be improved, as the pure Euclidian Norm used here is not very realistic by means of air traffic management and could be replaced by a more sophisticated distance path constraint.
Of course, aerial refueling in civil applications is in a very early stage of development and a lot of technological and safety issues have to be tackled before a technology readiness level could be achieved that would allow an implementation of such maneuvers into everyday procedures. Nevertheless, aerial refueling is quite well established in military applications and might also be used in other scenarios involving for example UAS or other modern – civil or military – flying equipment.

References

[1] Eurocontrol, "Long-Term Forecast, Flight Movements 2010-2030", www.eurocontrol.int, 2010.
[2] Nangia, R. K. 2006. Operations and aircraft design towards greener civil aviation using air-to-air refueling. In: The Aeronautical Journal, Vol. 110, Royal Aeronautical Society, London, 2006, 705ff.
[3] Nangia, R. K. 2006. Efficiency parameters for modern commercial aircraft. In: The Aeronautical Journal, Vol. 110.
[4] Nangia, R. K. 2008. Highly Efficient and Greener Civil Aviation - Organising a Step Jump towards ACARE Goals, An Opportunity for the Present & a Vision for Future Current Technology Trends. In: RAeS Conference Aerospace 2008, The Way Forward, London, April 2008.
[5] Green, J. E. 2001. Air Travel – Greener by Design, The Technology Challenge, Technical Report, RAeS, www.greenerbydesign.org.uk.
[6] Green, J. E. 2002. Greener by Design – the Technology Challenge. In: The RAeS Aeronautical Journal, Vol. 106, No.1056, February 2002, Erratum, Vol. 109, no 1092, 2005.

[7] Hahn, A. S. 2007. Staging Airliner Service. In: 7th AIAA ATIO Conference, 2nd CEIAT Int'l Conference on Innovation & Integration in Aero Sciences, 17th LTA Systems Technology Conference; followed by 2nd TEOS Forum, American Institute of Aeronautics and Astronautics, September 2007.
[8] N.N. 2012. User Manual for the Base of Aircraft Data (BADA) Revision 3.10, Eurocontrol Experimental Centre, No. 12/04/10-45, 2012.
[9] N.N.. 1975. The Standard Atmosphere, DIN ISO 2533, International Organization for Standardization, Genf, Schweiz, 1975.
[10] Torenbeek, E. 1988. Synthesis of Subsonic Airplane Design, Delft, Delft University Press.
[11] Raymer, D.P., 1989. Aircraft Design: A Conceptual Approach. AIAA Education Series, Washington D.C, AIAA.
[12] Roskam, J.. 1989. Airplane Design, Bd. 1-8, Ottawa, Kansas.
[13] Loftin, L.K. 1980. Subsonic Aircraft: Evolution and Matching of Size to Performance, NASA Reference Publication 1060.
[14] Airbus S.A.S. 2012. A380, Aircraft Characteristics – Airport and Maintenance Planning, Technical Documentation, AIRBUS S.A.S., Customer Services, Technical Data Support and Services, Rev. No. 11, Nov 2012.
[15] Betts, J. T. 1998. Survey of Numerical Methods for Trajectory Optimization", Journal of Guidance, Control, and Dynamics, Vol. 21, No. 2, pp. 193-207.
[16] Betts, J. T. 2012. Practical Methods for Optimal Control Using Nonlinear Programming, 2nd ed., SIAM: Advances in Design and Control, Philadelphia, Pennsylvania.
[17] Gill, P. E., Murray, W., and Saunders, M. A. 2007. User's Guide for SNOPT Version 7: Software for Large-Scale Nonlinear Programming, University of California, Department of Mathematics, San Diego, California.